Test-case number 23: Relative trajectories and collision of two drops in a simple shear flow (PA)

March 8, 2004

F. Pigeonneau, Saint-Gobain Recherche, BP 135, 39 quai Lucien Lefranc
93303 Aubervilliers cedex, France
Phone: +33 (0)1 48 39 59 99, Fax: +33 (0)1 48 39 58 78
E-Mail: *franck.pigeonneau@saint-gobain.com*

F. Feuillebois, PMMH, UMR 7636 CNRS, ESPCI, 10 rue Vauquelin
75231 Paris cedex 05, France
Phone: +33 (0)1 40 79 45 53, Fax: +33 (0)1 40 79 47 95
E-Mail: *francois.feuillebois@espci.fr*

N. Coutris, INPG/ENSPG and DER/SSTH/LMDL
CEA/Grenoble, 38054 Grenoble cedex 9, France
Phone: +33 (0)4 38 78 91 91, Fax: +33 (0)4 38 78 50 36
E-Mail: *coutrisni@chartreuse.cea.fr*

1 Practical significance and interest of the benchmark

Suspensions in gases, or aerosols, have applications in various domains like meteorology, nuclear and chemical engineering. In the Stokes regime of fluid motion, a moving drop in a flow creates hydrodynamic perturbations which interact with other drops. These interactions may lead to collisions and coalescence, thereby modifying the aerosol histogram. For small values of the volume fraction of the dispersed phase, the only significant hydrodynamic interactions are those between pairs of drops. This incentive to study the hydrodynamic interactions between two inclusions in a flow provides the aim of this test case.

The problem is restricted here to the motion of drops of equal size with initially spherical shape embedded in a simple shear flow. This kind of problem is essential for the formation of clouds Pruppacher & Klett (1978), Jonas (1996). The purpose is to study the relative trajectories and collision of the two drops in the Stokes flow regime.

The problem described in this paper has been solved analytically for non-deformable drops in the Stokes regime Pigeonneau. (1998), Pigeonneau & Feuillebois (2002). It will be of interest to compare these results with numerical simulations. Some numerical techniques may also go further and look at the deformation of drops (see *e.g.* Zapryanov & Tabakova, 1999), but this is outside the scope of the present benchmark.

2 Definitions and physical model description

2.1 Description, notation and assumptions

Consider two identical drops of radius a of the same material, embedded in a simple shear flow with velocity:

$$\boldsymbol{u}^{\infty}(\boldsymbol{x}) = \gamma z \boldsymbol{i}, \tag{1}$$

at a point $\boldsymbol{x}$. Here, γ denotes the shear rate and we use a system of rectangular coordinates (x, y, z), with $\boldsymbol{i}$ the unit vector along x. The unperturbed flow velocity and the two drops are represented in figure 1.

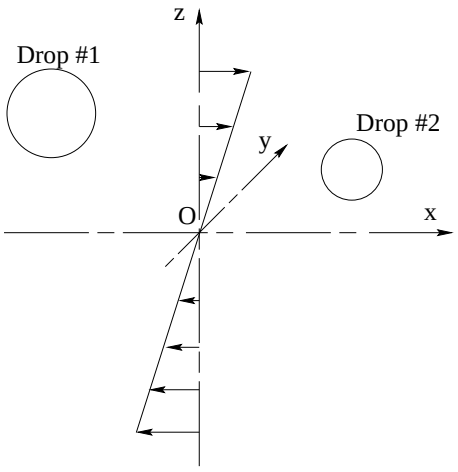

Figure 1: Schematic representation of two drops moving in simple shear flow.

The dispersed phase is denoted with a subscript L (for liquid) and the continuous phase with a subscript G (for gas). Let ρ be the density, η and ν the dynamic and kinematic viscosities respectively, with the relevant subscript for each phase. All these physical quantities are assumed to be constant. Let also

$$\hat{\rho} = \frac{\rho_L}{\rho_G} \tag{2}$$

be the density ratio and

$$\hat{\eta} = \frac{\eta_L}{\eta_G} \tag{3}$$

be the viscosity ratio.

The perturbed flows for the two phases and the motions of the two drops interfaces are described by Navier-Stokes equations. However here, we assume that the Reynolds numbers associated to the external and internal flows are low:

$$Re_G = \frac{\gamma a^2}{\nu_G} \ll 1\,; \qquad Re_L = \frac{\gamma a^2}{\nu_L} \ll 1$$

so that fluid inertia is negligible and Stokes equations apply. Note that the inertia in the drops motion may nevertheless be relevant, since the Stokes number St, defined by:

$$St = \frac{2}{9}\hat{\rho} Re_G, \tag{4}$$

may be of order unity. On the other hand, gravity will be ignored in the motion of the drops. The physical consistency of these assumptions is discussed in full detail in Pigeonneau & Feuillebois (2002).

The Reynolds numbers being low, the relevant non-dimensional number for the interfacial momentum balance is the capillary number:

$$Ca = \frac{\eta_G \gamma a}{\sigma}, \tag{5}$$

The surface tension σ is assumed to be constant here. Provided that the capillary forces are much larger than the viscous forces along the interface, viz. $Ca \ll 1$, the drops remain spherical during their motion. Note that for close drops, Chesters (1991) showed that their deformation is proportional to $\sqrt{Ca}$.

2.2 Formulation

Dimensionless quantities are defined in terms of a reference length a and a reference velocity γa. The dimensionless pressure p_G is defined in terms of the dimensional one p_G^* as:

$$p_G = \frac{p_G^*}{\gamma \eta_G}$$

and the dimensionless dynamic pressure p_L in terms of the dimensional pressure p_G^* and the pressure jump across the interface as:

$$p_L = \frac{2}{Ca} + \frac{p_L^*}{\gamma \eta_G}.$$

With these notations, the Stokes equations are written in dimensionless form in the continuous phase:

$$\begin{aligned} \mathrm{div}\boldsymbol{u}_G &= 0, & \text{(6a)} \\ \nabla^2 \boldsymbol{u}_G &= \mathbf{grad}\, p_G, & \text{(6b)} \end{aligned}$$

and in the dispersed phase :

$$\begin{aligned} \mathrm{div}\boldsymbol{u}_L &= 0, & \text{(7a)} \\ \hat{\eta}\nabla^2 \boldsymbol{u}_L &= \mathbf{grad}\, p_L. & \text{(7b)} \end{aligned}$$

Note that the time derivative of the fluid velocity is removed as the Reynolds numbers are vanishingly small in the Navier-Stokes equations. Thus, the equations are quasi-steady. The question of an initial condition for the flow field is irrelevant here, but the initial positions of the two drops have to be specified.

The boundary conditions on each drop interface are the continuity conditions for the fluid velocity

$$\boldsymbol{u}_G = \boldsymbol{u}_L, \qquad (8)$$

the continuity of the tangential stresses and the jump condition for the normal stresses:

$$\begin{aligned} \hat{\eta}\boldsymbol{\tau}_L \cdot \mathbb{D}_L \cdot \boldsymbol{n}_L &= \boldsymbol{\tau}_L \cdot \mathbb{D}_G \cdot \boldsymbol{n}_L, & \text{(9a)} \\ p_L - p_G &= \hat{\eta}\boldsymbol{n}_L \cdot \mathbb{D}_L \cdot \boldsymbol{n}_L - \boldsymbol{n}_L \cdot \mathbb{D}_G \cdot \boldsymbol{n}_L, & \text{(9b)} \end{aligned}$$

where $\mathbb{D}$ denotes the strain rate tensor, $\boldsymbol{n}_L$ is a unit vector normal to the interface, outwardly directed and $\boldsymbol{\tau}_L$ is a unit vector tangent to the interface.

Finally, the two flow fields outside and inside the moving drops are the solutions of the equations (6a-b), (7a-b), with the interfacial conditions (8) and (9a).

In Pigeonneau. (1998), Pigeonneau & Feuillebois (2002), the motion of the two interacting drops is determined in two steps. First, the drag forces on the two drops embedded in an unperturbed general linear flow field are obtained by using an exact solution of the Stokes equations with the bispherical coordinates system. Then, the study of the motions of their centers leads to the paths of the drops.

Scaling the forces with the quantity $6\pi\eta_G a^2\gamma$, the dimensionless drag forces on drops 1 and 2 are:

$$\boldsymbol{F}_1 = -\left\{\mathbb{A}_{11}\cdot[\boldsymbol{V}_1-\boldsymbol{u}^\infty(\boldsymbol{x}_1)]+\mathbb{A}_{12}\cdot[\boldsymbol{V}_2-\boldsymbol{u}^\infty(\boldsymbol{x}_2)]+\mathbb{G}_1:\mathbb{D}^\infty\right\}, \tag{10a}$$

$$\boldsymbol{F}_2 = -\left\{\mathbb{A}_{21}\cdot[\boldsymbol{V}_1-\boldsymbol{u}^\infty(\boldsymbol{x}_1)]+\mathbb{A}_{22}\cdot[\boldsymbol{V}_2-\boldsymbol{u}^\infty(\boldsymbol{x}_2)]+\mathbb{G}_2:\mathbb{D}^\infty\right\}. \tag{10b}$$

where $\boldsymbol{x}_1$ and $\boldsymbol{x}_2$ are the positions of the drops centers, $\boldsymbol{V}_1$ and $\boldsymbol{V}_2$ are their velocities. The detailed expressions of the second rank tensors $\mathbb{A}_{11}$, $\mathbb{A}_{12}$, $\mathbb{A}_{21}$, $\mathbb{A}_{22}$ and the third rank tensors $\mathbb{G}_1$ and $\mathbb{G}_2$ are detailed in Pigeonneau. (1998), Pigeonneau & Feuillebois (2002).

Scaling the time t with γ^{-1}, the dimensionless equations leading to the motion of the drops can be written as:

$$\frac{d\boldsymbol{x}_1(t)}{dt} = \boldsymbol{V}_1, \tag{11a}$$

$$\frac{d\boldsymbol{x}_2(t)}{dt} = \boldsymbol{V}_2, \tag{11b}$$

$$St\frac{d\boldsymbol{V}_1(t)}{dt} = \boldsymbol{F}_1, \tag{11c}$$

$$St\frac{d\boldsymbol{V}_2(t)}{dt} = \boldsymbol{F}_2. \tag{11d}$$

	Quantity	Value	Unity
Shear rate	γ	10^3	s^{-1}
Radius	a	10^{-5}	m
	ρ_L	1000	kg/m^3
Water	η_L	$1.787\cdot10^{-3}$	Pa.s
	ν_L	$1.787\cdot10^{-6}$	m^2/s
	ρ_G	1.29	kg/m^3
Air	η_G	$1.71\cdot10^{-5}$	Pa.s
	ν_G	$1.325\cdot10^{-5}$	m^2/s
Surface tension	σ	$7.61\cdot10^{-2}$	N/m

Table 1: Selected values of the physical properties of water and air.

3 The description of the benchmark

3.1 Input parameters and physical properties

The method described above can be used to study the motion of water drops in air. The value of the shear rate of the unperturbed flow velocity (1) is taken as $\gamma = 10^3$ s^{-1}. The drops radius is $a = 10$ μm. Selected values of the physical properties of water and air and of the surface tension between air and water are given in table 1. Values of the dimensionless numbers for this set of data are given in table 2. Both the Reynolds numbers and capillary number are small. Consequently, the Stokes regime for each phase is relevant. The assumption of non-deformable drops is also justified by the small value of the capillary number.

Number	Value
Re_G	$7.55 \cdot 10^{-3}$
Re_L	$5.59 \cdot 10^{-2}$
Ca	$2.25 \cdot 10^{-6}$
St	1.3
$\hat{\eta}$	104.5
$\hat{\rho}$	775.19

Table 2: Values of the dimensionless numbers.

3.2 Initial conditions

Initially, the drops are embedded in the flow field, the distance between their centers being equal to ten times their radius a. The velocities of the drops are initialized to zero. These initial conditions are summarized in table 3, where u, v, z denote the components of the velocity in the Cartesian reference frame (x, y, z).

	Position			Velocity		
	x	y	z	u	v	w
Drop 1	-5	0	0	0	0	0
Drop 2	5	0	0	0	0	0

Table 3: Initial positions and velocities of the two drops.

3.3 Results and comparisons

The two centers remain in the plane Oxz. Nevertheless, the flow problem is three-dimensional. A very important point concerns the forces on the drops in their initial positions: the only non-zero component is along the z axis. This can be proven as in Bretherton (1962) using the linearity and reversibility of the Stokes equation. The forces on drops 1 and 2 are opposite, the force on drop 1 being z-directed, their values are deduced from the results obtained in Pigeonneau. (1998), Pigeonneau & Feuillebois (2002) are

$$F_{1z} = -F_{2z} = 1.4221 \cdot 10^{-4}. \tag{12}$$

Using the analytical solution, it is shown in Pigeonneau. (1998), Pigeonneau & Feuillebois (2002) that the drops collide at the positions defined in table 4 at the dimensionless time $t = 186.49$. The trajectories of the drops are shown in figure 2. These trajectories are symmetric with respect to the origin of the Cartesian reference frame. One of the reasons is that the drops have the same radius. The dimensionless coordinates at different times are given in table 4.

4 Conclusion

The challenge is to recover the drops trajectories for the physical data mentioned above. There are various ways to compute a solution. One of them could be *e.g.* the boundary integral method for Stokes flow.

	Drop 1		Drop 2	
t	x_1	z_1	x_2	z_2
0	-5	0	5	0
9.161	-4.997	$1.050 \cdot 10^{-3}$	4.997	$-1.050 \cdot 10^{-3}$
91.793	-4.436	$1.393 \cdot 10^{-2}$	4.436	$-1.393 \cdot 10^{-2}$
173.62	-2.010	$7.981 \cdot 10^{-2}$	2.010	$-7.981 \cdot 10^{-2}$
184.01	-1.005	$2.797 \cdot 10^{-1}$	1.005	$-2.797 \cdot 10^{-1}$
185.08	-0.914	0.415	0.914	-0.415
186.39	-0.710	0.704	0.710	-0.704
186.45	-0.695	0.719	0.695	-0.719
186.49	-0.681	0.732	0.681	-0.732

Table 4: Drop coordinates at various times.

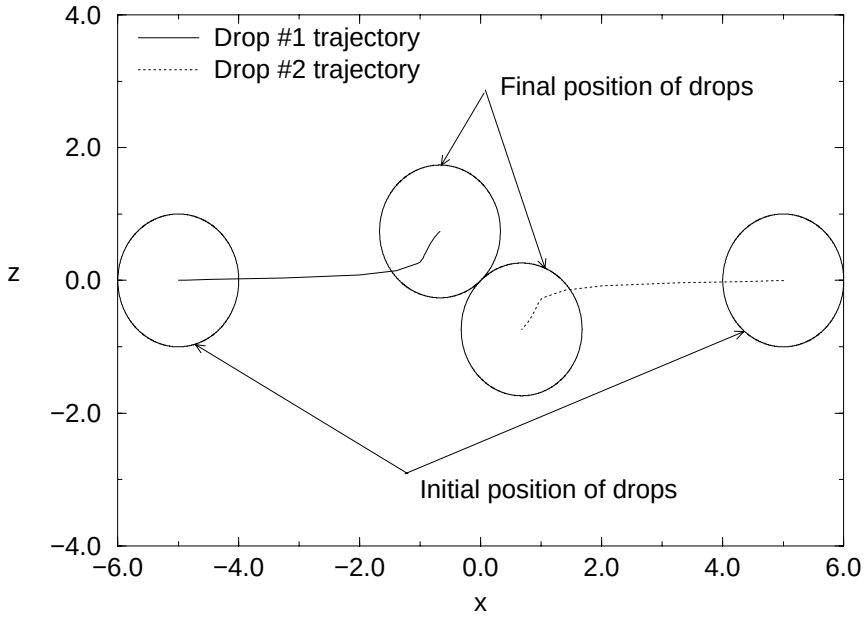

Figure 2: Trajectories of the drops from initial to final positions.

References

Bretherton, F. P. 1962. The motion of rigid particles in a shear flow at low Reynolds number. *J. Fluid Mech.*, **14**, 284–304.

Chesters, A. K. 1991. The modelling of coalescence processes in fluid-liquid dispersions: A review of current understanding. *Trans. Instn. Chem. Engrs.*, **69**, 259–270.

Jonas, P. R. 1996. Turbulence and cloud microphysics. *Atmospheric Research*, **40**, 283–306.

Pigeonneau., F. 1998. *Modélisation et calcul numérique des collisions de gouttes en écoulements laminaires et turbulents*. Ph.D. thesis, Université Pierre et Marie Curie, Paris VI.

Pigeonneau, F., & Feuillebois, F. 2002. Collision of drops with inertia effects in strongly sheared linear flow fields. *J. Fluid Mech.*, **455**, 359–386.

Pruppacher, H. R., & Klett, J. D. 1978. *Microphysics of clouds and precipitation*. D. Reidel publishing company.

Zapryanov, Z., & Tabakova, S. 1999. *Dynamics of bubbles, drops and rigid particles*. Kluwer academic publishers, Dordrecht.